Molecular Vision 2018; 24:1-16 <http://www.molvis.org/molvis/v24/1>
Received 11 August 2017 | Accepted 2 January 2018 | Published 4 January 2018

Full-field ERG as a predictor of the natural course of *ABCA4*-associated retinal degenerations

Marion Schroeder, Ulrika Kjellström

Lund University, Skane University Hospital, Department of Clinical Science Lund, Ophthalmology, Lund, Sweden

Purpose: To assess retinal function in combination with the retinal structure in *ABCA4*-associated retinal degenerations. Moreover, to evaluate the possibility of predicting the natural course of these disorders.

Methods: 34 patients with Stargardt disease or cone rod dystrophy carrying confirmed mutations in *ABCA4* were selected from our retinitis pigmentosa (RP) register. Sequence analysis of the entire coding region of the *ABCA4* gene was performed. The patients were subdivided into three groups based on their most recent visual fields. Group 1 included ten patients with central scotomas within 10°, group 2 included 19 patients with larger central scotomas of 10–35°, and group 3 included five patients with mere temporal residues. The patients underwent slit-lamp and fundus examinations, visual acuity testing, optical coherence tomography (OCT), fundus photography (color, red-free, and autofluorescence (AF) images), full-field electroretinography (ffERG), and multifocal electroretinography (mERG). FfERG and mERG results were analyzed statistically. Total rod and cone function, as well as macular function, was compared between the three groups and of each group to a normal material. In 23 patients who had undergone ffERG on a previous occasion, the 30 Hz flicker implicit time (IT) from the first visit was also analyzed.

Results: The ffERG statistics revealed significant differences between the groups regarding cone and rod function with group 1 showing the highest amplitudes and the shortest ITs while group 3 demonstrated the lowest amplitudes and the most delayed ITs. When compared to controls, group 1 did not show any significant changes while groups 2 and 3 demonstrated reduced amplitudes and delayed 30 Hz ITs. Regarding estimation of the natural course, identical results of the 30 Hz IT were encountered for the groups also at the first visit early in the course of disease. Comparison of the mERGs showed significant differences with group 1 demonstrating the highest amplitudes and group 3 the lowest for all rings but rings 2 and 3 in the right eye for which the amplitudes were the second highest. The mERGs for each group were also compared to controls showing reduced mERG amplitudes for all rings in all groups, except group 1, left eye. OCT showed macular attenuation in all patients. Evaluation of the inner and outer photoreceptor junction (IS/OS) morphology revealed alterations related to macular function measured with mERG in all eyes. Eight patients in group 1 showed foveal IS/OS junction loss, one had foveal IS/OS junction disorganization, and one had IS/OS loss also beyond the fovea. In group 2, one patient had IS/OS junction loss confined to the fovea, and the rest showed total loss of IS/OS junctions. Group 3 was devoid of IS/OS junctions. Concerning the AF images, group 1 showed small areas of absent AF in the macula, peripapillary sparing, and flecks of increased and reduced AF in the posterior pole. In group 2, the central areas of absent AF were larger. Flecks of reduced AF were the most dominant and reached beyond the posterior pole. Seven of 19 patients had peripapillary sparing. In group 3, large confluent areas of reduced AF were found in the posterior pole and beyond with small areas of increased AF in the far periphery. No peripapillary sparing was seen.

Conclusions: The current study demonstrates a significant difference in total retinal function, as well as macular function, between patients with *ABCA4*-associated retinal degeneration and a different degree of visual field defects with gradual deterioration of function along with increased visual field constriction. Likewise, the morphological changes, including the deviant AF pattern and loss of IS/OS junctions, that were related to macular function measured with mERG worsened with the degree of visual field defects. Moreover, in these groups of patients with *ABCA4*-associated retinal degenerations, full-field cone 30 Hz flicker IT seems to be a predictor of the natural course of the disease also on long-term follow-up.

ABCA4-associated retinal degenerations are severe recessively hereditary disorders that lead to a wide range of visual symptoms and handicaps. The underlying causes are compound heterozygous or homozygous mutations in the *ABCA4* gene, a large (128 kbp) gene on chromosome 1 (1p22.1) OMIM that encodes the ABCA4 protein. ABCA4 is a membrane-associated transporter protein located in the rim of the discs in the outer segments of the rods and cones [1-3]. The ABCA4 protein belongs to the group of ATP binding cassette (ABC) transporter proteins, a superfamily of proteins that actively transfer biologic compounds, such as polypeptides, amino acids, lipids, and vitamins, across cell membranes [4]. In photoreceptors, the ABCA4 protein clears the toxic retinoid compounds N-retinylidenephosphatidylethanolamine

Correspondence to: Ulrika Kjellström, Ögonkliniken Skånes Universitetssjukhus Lund, S 221 85 Lund, Sweden; Phone: +46-70-566 52 54; FAX: +46-46-13 90 45; email: ulrika.kjellstrom@med.lu.se

(NRPE) and phosphatidylethanolamine (PE) from the interior of the outer segment discs to the cytosol after photobleaching of the opsins during the phototransduction cascade [5-7]. Failure of this clearing process eventually leads to accumulation of lipofuscine fluorophores, for example, N-retinylidene-N-retinylethanolamine (A2E), in RPE cells [7-9] and over time to RPE cell death and secondary loss of photoreceptors [7,10]. Some authors [11-13] also have suggested that direct photoreceptor cell death may precede the pathological process in the RPE.

The severity of *ABCA4*-associated retinal degenerations can vary considerably. The most common variant is Stargardt disease (STGD) typically starting in late childhood or the early teens causing juvenile onset macular degeneration with reduced visual acuity (VA), central scotomas, and photophobia [14-17]. Fundus examination can be quite normal in the beginning of the course of the disease, but over time, symmetric, bilateral, atrophic changes in the RPE and orange-yellow spots in the macular region and midperiphery are encountered [14]. Mutations in *ABCA4* also can be associated with cone-rod dystrophy (CRD) [18-21], an even more severe type of retinal degeneration with a more aggressively progressive course, initially engaging cones leading to reduction of VA, reduced color vision, and central, as well as paracentral, scotomas. Over time, rods also degenerate with night blindness and peripheral visual field constriction as a result. Fundus changes might be less typical with unspecific pigmentations in the macula and in the midperiphery [21,22]. More seldom, mutations in *ABCA4* cause autosomal recessive retinitis pigmentosa (arRP) [19,22,23] with early symptoms of reduced night vision and peripheral visual field constriction followed by reduced VA, central scotoma, photophobia, and reduced color vision. In some cases, fundus changes are typical for RP with a pale optic disc, attenuated retinal vessels, and peripheral bone spicule-like pigmentations, but sometimes, merely unspecific atrophy is found [24]. At the moment, around 1,000 mutations, possibly or definitely [25], causing retinal degeneration have been identified in the *ABCA4* gene. Due to the many possible combinations of mutations, it is difficult to predict the type of retinal degeneration from the mutations only, although many attempts have been made to correlate the severity of disease to the estimated effect of individual mutations on gene transcription and translation of the ABCA4 protein [26-29].

Concerning STGD and CRD, differentiating between these two entities can be hard in the beginning of the course of the disease, because both conditions start with similar symptoms of reduced VA and central scotoma, although CRD is a more progressive disorder leading to more severe visual handicaps in the long run. Thus, the final visual outcome for the individual patient can be different, and parameters that can help in making a correct prognosis are very welcome. Therefore, in this survey, we wanted to study patients with genetically defined *ABCA4*-associated retinal degenerations with different degrees of visual field defects to investigate differences in retinal morphology, as well as electrophysiological parameters reflecting retinal function.

METHODS

Subjects: At the start of the study, all (n=37) patients with confirmed homozygous or compound heterozygous mutations in *ABCA4* that were identified in our RP register at the Department of Ophthalmology, Skåne University Hospital, Lund, Sweden were invited to participate. 34 patients (20 women and 14 men) previously diagnosed with either STGD or CRD consented to take part. Two patients with CRD, according to the records, declined to participate, and another patient with CRD could not be reached. The mean age of the participants was 34 years (range: 10–71 years). The patients were further subdivided into three groups based on the most recent results of their Goldmann visual fields. Group 1 included ten patients aged 18–71 years (mean 37.5) with only small central scotomas within 10°. Group 2 included 19 patients aged 10–61 (mean 29) that had larger scotomas from 10° to 35°, and group 3 comprised five patients aged 23–70 years (mean 43) with widely aberrant visual fields with merely some peripheral temporal crescent-formed residuals left. Demographic data for the patients are presented in Table 1, and typical examples of the visual fields are shown in Figure 1. Short descriptions of the distribution of visual field defects are given in Appendix 1. The study was conducted in accordance with the Tenets of the Declaration of Helsinki and adhered to the ARVO statement on human subjects. All subjects gave their written consent to participate in the study that was approved by the Ethical Committee for Medical Research at Lund University.

Control groups: For comparison of the full-field electroretinography (ffERG) parameters, a control group consisting of 46 healthy persons aged 10–62 years (mean 35 years) was used. Another control group of 44 healthy persons aged 10–64 years (mean 37 years) was employed to compare the multifocal electroretinography (mERG) data.

Ophthalmological examination and genetic analysis: Best-corrected monocular Early Treatment Diabetic Retinopathy Study (ETDRS) visual acuity (VA) was tested at 1, 2, or 4 m, and the ETDRS visual acuity score was calculated for each eye. Moreover, Goldmann perimetry was performed using standardized objects V4e and I4e. In some patients,

Table 1. Demographic data, *ABCA4* mutations, and ffERG results.

Subject/ Age/Group Age at first ffERG/ Gender	Original diagnosis from the records	*ABCA4* mutations	ETDRS VA score (RE, LE)	Rod ffERG (RE, LE) Ampl (μV)	Combined ffERG (RE, LE) Ampl (μV)	Cone ffERG (RE, LE) Amp IT (μV; ms)		mERG sum (RE, LE) Ampl (μV)
1/41/**1**/29/ male	STGD	c.4773+3A>G (hom)	86, 90	279, 268	430, 425	59, 61	31.0, 31.5	27, 23
2/71/**1**/NRP/ female	STGD	c.2564 G>A c.3113 C>T c.4506 C>T	13, 77	164, 159	283, 284	35, 41	38.0, 37.0	6, 9
3/27/**1**/20/ female	STGD	c.1622 T>C c.3113 C>T c.5882 G>A	44, 43	294, 299	488, 522	80, 81	27.0, 26.5	20.7, 23.7
4/48/**1**/NRP/ male	STGD	c.5882 G>A c.5917del	74, 64	165, 144	356, 334	57, 55	28.5, 28.5	20.7,
5/45/**1**/21/ female	STGD	c.3113 C>T c.768 G>T	43, 44	195, 154	367, 315	59, 54	28.0, 27.5	12.4, 9.6
6/34/**1**/NR/ female	STGD	c.768 G>T c.1610 G>A	N, N	216, 230	320, 451	89, 96	27.5, 28.6	N
7/38/**1**/30/ female	STGD	c.2915 C>A c.5537 T>C	39, 41	388, 306	657, 524	95, 83	30.0, 30.0	28.4, 21.7
8/18/**1**/NRP female	STGD	c.868 C>T c.317 A>T	N, N	252, 238	348, 260	73, 49	27.0, 27.5	25.0, 24.8
9/32/**1**/29 female	STGD	c.3386 G>T (hom)	68, 68	285, 224	433, 378	68, 64	31.0, 30.5	18.0, 24.7
10/22/**1**/NRP female	STGD	c.5882 G>A c.5917del	39, 40	277, 230	371, 309	75, 60	27.5, 27.5	24.4
11/35/**2**/22 male	STGD	c.2588 G>C c.4253+4 C>T	N, N	269, 223	470, 369	87, 74	30.5, 30.5	11.3, 17.7
12/10/**2**/NRP male	STGD	c.768 G>T (hom)	49. 54	119, N	199, N	29, N	30.5, N	8.2, N
13/23/**2**/17 male	CRD	c.1622 T>C c.3113 C>T c.1804 C>T	30, 25	48, 38	136, N	9, 11	46.0, 50.0	2.2, N
14/39/**2**/NRP/ female	CRD	c.1933 G>T c.4249_4 251del	N, N	43, 65	N, N	21, 32	40.0, 39.5	5,7 N
15/29/**2**/19 female	CRD	c.5882 G>A c.4773+1 G>A	24, 21	17, 17	23, 18	2, 7	42.0, 39.6	1.3 1.7

Subject/ Age/Group Age at first ffERG/ Gender	Original diagnosis from the records	*ABCA4* mutations	ETDRS VA score (RE, LE)	Rod ffERG (RE, LE) Ampl (μV)	Combined ffERG (RE, LE) Ampl (μV)	Cone ffERG (RE, LE) Amp IT (μV; ms)		mERG sum (RE, LE) Ampl (μV)
16/40/**2**/32 male	CRD	c.286 A>G c.1798 G>T	15, 9	108, 116	215, 191	44, 61	35.0, 33.0	7.3, 10.3
17/41/**2**/17/ male	STGD	c.768 G>T c.6112 C>T	6, 25	83, 103	153, 175	19, 24	36.0, 34.0	6.0, 9.3
18/40/**2**/20/ female	STGD	c.2588 G>C c.4253+4 C>T	N, N	132, 81	241, 144	37, 24	35.0, 39.5	9.7, 9.3
19/27/**2**/NRP/male	CRD	c.634 C>T c.5882 G>A	N, N	81, 63	158, 123	19, 26	34.5, 34.0	8.6
20/28/**2**/18/ female	CRD	c.1654 G>A c.4363 T>C	35, 35	38, 34	52, 57	4, 5	45.0, 42.5	1.0, 0.7
21/27/**2**/16/ female	STGD	c.768 G>T (hom)	13, 28	62, 42	71, 91	4, 4	42.0, 42.5	1.0, 1.3
22/16/**2**/7/ male	CRD	c.319 C>T c.5461–10 T>C	N, N	69, 61	104, 85	7, 6	45.4, 45.5	N, 1.7
23/20/**2**/13/ female	CRD	c.768 G>T c.2894 A>G	20, 22	168, 144	225, 234	11, 13	42.1, 39.5	2.3, 2.3
24/16/**2**/NRP/ female	STGD	c.1622 T>C c.3113 C>T c.1804 C>T	11, 17	178, 170	452, 290	32, 35	36.0, 35.0	3.8, N
25/31/**2**/26/ female	STGD	c.4773+1 G>A c.53 G>A	17, 22	101, 131	153, 181	16, 48	39.5, 39.0	2.0, 4.3
26/25/**2**/12/ male	STGD	c.2894 A>G (hom)	19, 24	143, 134	260, 280	31, 41	29.5, 28.5	8.7, 13.7
27/22/**2**/18/ female	STGD	c.2894 A>G c.4667+ T>C	17, 36	162, 122	270, 214	59, 79	33.5, 33.0	3.8, 4.5
28/24/**2**/19/ female	CRD	c.768 G>T c.2894 A>G	14, 23	145, 162	290, 252	23 27	38.0, 39.5	N, N
29/62/**2**/NRP/ male	STGD	c.1007 C>G c.5714+ 5G>A	N, N	33, 57	N, N	9, 14	42.0, 42.0	N, N
30/23/**3**/17/ male	CRD	c. 5917 del (hom)	17, 24	60, 75	101, 103	12, 13	40.0, 41.0	N, 1.3
31/50/**3**/NRP/ female	CRD	c.768 G>T c.4253+ 4C>T	4, 3	72, 70	104, 109	6, 7	41.2, 43.2	3.3, 1.7
32/40/**3**/36/ male	CRD	c.3259 G>A (hom)	0, 4	30, 4	40, 29	4, 2	43.5, 42.0	Not measurable

Subject/ Age/Group Age at first ffERG/ Gender	Original diagnosis from the records	*ABCA4* mutations	ETDRS VA score (RE, LE)	Rod ffERG (RE, LE) Ampl (μV)	Combined ffERG (RE, LE) Ampl (μV)	Cone ffERG (RE, LE) Amp IT (μV; ms)		mERG sum (RE, LE) Ampl (μV)
33/34/**3**/32/ male	CRD	c.6229 C>T (hom)	6, 16	39, 36	76, 67	9, 13	43.0, 43.5	5.7, 3.3
34/70/**3**/63/ female	CRD	c.768 G>T c.2894 A>G	N, N	10, 0	N, N	6, 7	41.0, 41.0	N, N

BVA=best corrected visual acuity, ETDRS=early treatment diabetic retinopathy study, RE=right eye, LE=left eye, Ampl=amplitude, μV=micro volt, IT=implicit time, ms=milliseconds, STGD=Stargardt disease, hom=homozygote, NRP=not registered previously, n=not performed, CRD=cone-rod dystrophy

Molecular Vision 2018; 24:1-16 <http://www.molvis.org/molvis/v24/1>

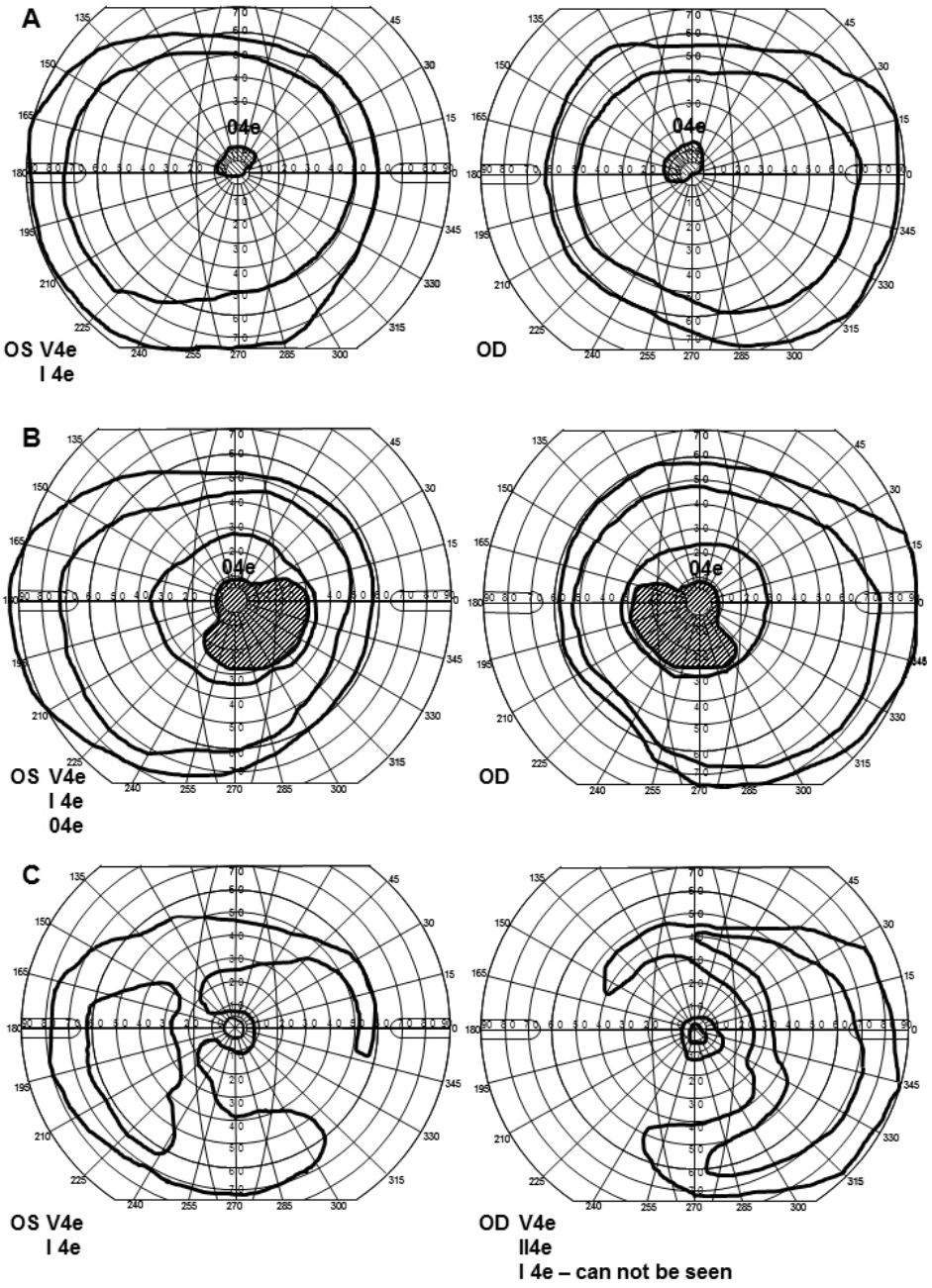

Figure 1. Examples of Goldmann visual field plots from one patient in each of the three groups. **A**: Typical Goldmann visual fields for group 1 with small central scotomas less than 10° (patient 10). **B**: Group 2 with larger central scotomas from 10° to 35° (patient 24). **C**: Typical for group 3 with temporal visual field residues (patient 30).

04e, 03e, 02e, and 01e were also tested. Fundus photographs including red-free photographs, color photographs, and fundus autofluorescence (FAF) images were captured with a Topcon TRC 50DX fundus camera (Topcon, Inc., Oakland, NJ). For the AF images, the field of view was 50 × 50°, and Spaide filters (Topcon, Inc.) with an excitation wavelength of 530–580 nm and a barrier filter of 600–720 nm were used. All patients also had detailed fundus and slit-lamp examinations. Sequence analysis of the entire coding region of the *ABCA4* gene was performed at Asper Biotech (Asper Ophthalmics, Tartu, Estonia).

Statistical analysis: All statistical calculations were made in SPSS 22 (IBM SPSS Statistics, IBM Corporation, Chicago, IL). A p value of less than 0.05 was considered statistically significant. To compare the ffERG and mERG parameters between the three visual field groups, the Kruskal–Wallis test was used. To compare the ffERG and mERG parameters in the separate visual field groups to the normal material, the Mann–Whitney U-test was applied. Nonparametric tests were used because the groups were small, and ERG parameters can have a slightly skewed distribution.

Full-field electroretinography: FfERGs were collected with an Espion E^2 analysis system (Diagnosys, Lowell, MA). Full-field electroretinograms were recorded according to the standardized protocol for clinical electroretinography recommended by the International Society for Clinical Electrophysiology of Vision (ISCEV) [30,31]. A Burian-Allen bipolar ERG contact lens electrode (Hansen Ophthalmic Development Lab, Coralville, IA) was used, and measurements were finished after 40 min of dark adaptation with maximally dilated pupils (cyclopentolate 1% and phenylephrine hydrochloride 10%). To ensure reproducibility, the recordings were repeated for all stimulus intensities until two successive identical curves were obtained. In 23 of the patients, older ffERG registrations were also reviewed. They were collected with a Nicolet Viking analysis system (Nicolet Biomedical Instruments, Madison, WI) using the same standards and settings.

Multifocal electroretinography: The Visual Evoked Response Imaging System (VERIS Science 6; EDI, San Mateo, CA) was used to record the mERGs. Settings that adhere to the ISCEV guidelines [30] were applied using a stimulus matrix consisting of 103 hexagons scaled with eccentricity to produce equal amplitudes of the responses all over the matrix. Hexagons independently altered between white and black according to a pseudorandom binary m-sequence at 75 Hz. Recordings were registered with a Burian-Allen bipolar ERG contact lens electrode. Pupils were maximally dilated with cyclopentolate 1% and phenylephrine chloride 10%. Proper central fixation was monitored with an infrared (IR) eye camera mounted in the mERG equipment, and the investigator continuously checked that the patient kept on fixating centrally. The first-order component of the mERG was analyzed regarding the amplitude (A) and the implicit time (IT) of the first positive peak (P1) within the five concentric rings (A 1–5 and IT 1–5) around the fovea. Ring 1, the innermost ring, represents the summed responses from the center and the first ring. The summed amplitudes and the implicit times of the mERG rings were also registered.

Optical coherence tomography: A spectral domain-based optical coherence tomography (OCT) Topcon 3D OCT-1000 (Topcon, Inc., Paramus, NJ) was used to capture three-dimensional (3D) OCT scans with a scan size of 6 × 6 mm and a scan density of 512 × 128. The internal fixation target (preset for macular imaging) was applied. Macular thickness was measured using the standard retinal thickness map of the OCT software (version 3.51 or 8.11). The map was composed of three concentric circles with diameters 1, 3, and 6 mm, respectively. The two outer circles were subdivided into four segments each, corresponding to the superior, nasal, inferior, and temporal segments. In this study, the segments were designated as follows (Appendix 1): central circle; segment 1, inner superior segment; 2, inner temporal segment; 3, inner inferior segment; 4, inner nasal segment; 5, outer superior segment; 6, outer temporal segment; 7, outer inferior segment; 8 and outer nasal segment; 9. For each segment of the retinal map, the mean retinal thickness, from the RPE to the inner limiting membrane (ILM), was measured. The mean thickness of each segment was also automatically compared to age-matched normative data, and deviant results were indicated. Retinal thickness was considered pathologically attenuated when values below the fifth percentile of the normative data were found. Similarly, the retina was considered pathologically thickened if values beyond the 95th percentile were encountered. Cross-sectional macular morphology was also studied on B-scan images.

RESULTS

Ophthalmological examination: Demographic data, original diagnosis, mutations in *ABCA4*, the ETDRS VA score, and electrophysiological data are presented in Table 1. A separate description of the distribution of the visual field defects and the OCT findings are shown in Appendix 1. All patients had abnormal fundus examinations showing subtle (pigmentary irregularity in the macular region) to extensive retinal changes (pale optic discs, narrowed retinal vessels, atrophies, deep yellowish flecks, and pigmentations). In group 1, eight of the patients had macular pigmentary changes only, while two patients (1 and 7) also had deep yellow flecks, either in the posterior pole (7) or in the posterior pole and beyond the vascular arcades (1). In group 2, all patients had extensive atrophies in the posterior pole. In addition, three patients (11, 24, and 27) had central and peripheral yellow flecks, and ten patients (12, 15, 16, 18, 20, 21, 23, 25, 26, and 28) demonstrated peripheral and sometimes also central (15, 16, and 18) pigmentations. In group 3, four patients (30–33) displayed marked atrophy in the macular region and bone corpuscle pigmentations within and outside the vascular

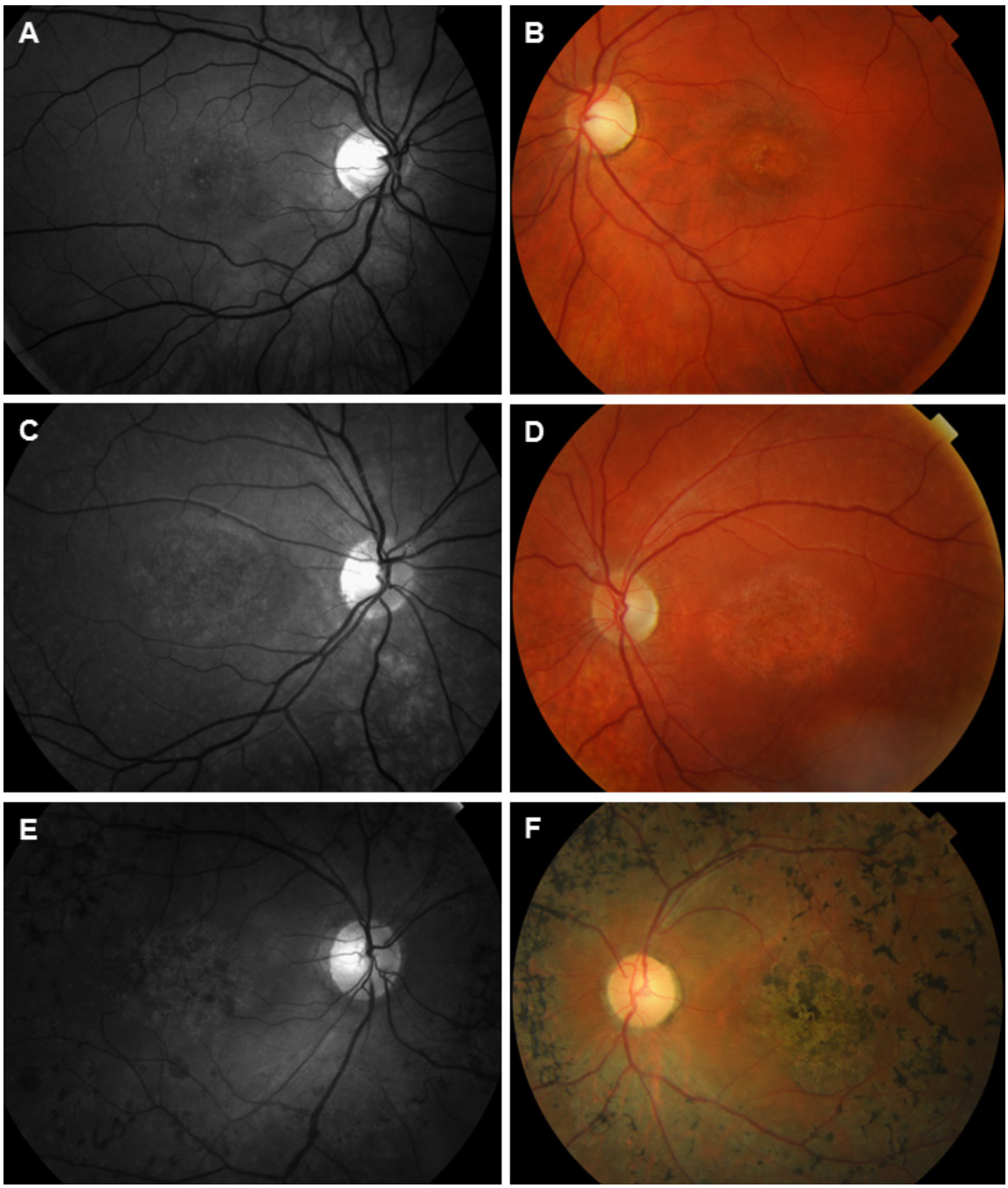

Figure 2. Representative red-free and color fundus photographs of patients from the three groups. **A** and **B**: Patient 10 in group 1 shows subtle pigmentary irregularity in the macular region as in most patients in the group. **C** and **D**: Subject 24 in group 2 demonstrates a slightly pale optic disc, more widespread pigmentary changes in the posterior pole, as well as deep yellow flecks in the midperiphery; in this subject most apparent nasal and inferior of the optic nerve. More extensive flecks were encountered in some other subjects in the group. **E** and **F**: Patient 30 reveals a pale optic disc, narrow retinal vessels, extensive pigmentary changes in the macular region, and bone corpuscle pigmentations in the periphery.

arcades. Patient 34 demonstrated the same central pathology but more unspecific pigmentations. Three of the patients (31, 33, and 34) also had attenuated vessels and a pale optic nerve head. Examples of fundus photographs from one patient of each group (patients 10, 24, and 30) are shown in Figure 2.

Autofluorescence images: We have complete AF data sets in eight of ten patients in group 1, 15 of 19 in group 2, and four of five in group 3. The findings showed a range of AF patterns comparable to those found by Sodi et al. [32] with the main focus on the following features: flecks with high or low AF, multiple foci of diffuse AF or multiple confluent foci of reduced AF in the macula, absence of AF within the macula, macular changes surrounded by a ring of high AF, and peripapillary sparing. Loss of peripapillary sparing was defined as the presence of any changes in the background AF, lower or higher values, in the peripapillary retina.

In group 1, seven out of eight patients with AF images presented with small areas of absent AF in the macular region, indicating macular atrophy, confirmed with the color fundus photographs and OCT. One patient (10) showed no absence but multiple foci of reduced AF in the macular region. A complete ring of high AF surrounding the macular changes was seen in three patients with low and high AF changes limited to the posterior pole (3, 9, and 10). All patients had flecks with high and low intensity of AF in the posterior pole, some even beyond. Of the latter were two patients (1 and 2) with a great number of flecks beyond the retinal vascular arcades. All patients showed peripapillary sparing.

Group 2 showed a wider range of phenotypes with AF changes somewhat in between groups 1 and 3. Five patients (12, 15, 16, 17, and 25) had developed large areas of absence of AF in the macula whereas three patients (11, 26, and 27) showed small lesions. In general, these areas were larger than in group 1. The majority of patients demonstrated multiple confluent loci of reduced AF at the posterior pole, with one exception (17). In contrast to group 1, group 2 presented with predominantly flecks of low AF. Eight of 15 patients (11, 12, 13, 15, 18, 21, 24, and 28) had no peripapillary sparing, five patients (16, 20, 23, 25, and 27) presented with few peripapillary changes, and two patients (17 and 26) with peripapillary sparing.

In group 3, all but one patient (30) showed huge areas with a total absence of AF reaching beyond the posterior pole, even nasally, without peripapillary sparing. Moreover, the patients often presented flecks with high and low values of AF in the midperiphery. Examples of AF images from one patient of each group are presented in Figure 3.

Full-field electroretinography: The Kruskal–Wallis test showed statistically significant differences in the ffERG results between the three groups concerning the isolated rod b-wave amplitude, combined rod-cone a-wave amplitude, combined rod-cone b-wave amplitude, isolated cone 30 Hz flicker amplitude, and isolated cone 30 Hz flicker implicit time ($p<0.0001$ for all parameters in the right and left eyes). Group 1 demonstrated the highest amplitudes and the shortest implicit times, while group 2 showed the second highest amplitudes and the second shortest implicit times, and group 3 the lowest amplitudes and the longest implicit times (see Table 2 for the means and standard deviations (SDs)). The ffERG data for each group were also compared to the ffERG data for the control group (the Mann–Whitney U-test). For group 1, no statistically significant differences were found ($p>0.05$ for all parameters). For groups 2 and 3, the isolated rod b-wave amplitude was statistically significantly reduced ($p<0.0001$), as well as the combined rod-cone a- and b-wave amplitudes and the cone 30 Hz flicker amplitude ($p<0.0001$ for all parameters). Moreover, the cone 30 Hz flicker implicit time was statistically significantly delayed for both groups ($p<0.0001$).

23 of the patients had undergone ffERG measurements 2–24 years before the current registrations (five patients in group 1, 14 patients in group 2, and four patients in group 3). The 30 Hz flicker implicit times for these initial ffERG measurements were also compared to the normal material (the Mann–Whitney U-test) showing significantly delayed cone 30 Hz flicker implicit times in groups 2 and 3 at the first ffERG registration (group 2; $p=0.009$ RE, $p<0.0001$ LE, group 3; $p=0.001$ RE and LE). In group 1, no statistically significant changes in the cone 30 Hz flicker implicit times were found ($p>0.05$) when the results at the first visit were compared to the normal material. The means and standard deviations for the 30 Hz cone flicker implicit times of each group at the first visit (1-3) are shown in Table 2.

Multifocal electroretinography: The Kruskal–Wallis test revealed statistically significant differences in the mERG amplitudes among the three groups concerning all rings (1–5) in both eyes. Group 1 demonstrated the highest amplitudes for all rings in both eyes. Group 2 showed the second highest amplitudes for all rings but rings 2 and 3 in the right eye for which the amplitude was lower than for group 3. Correspondingly, group 3 demonstrated the lowest amplitudes for all rings but rings 2 and 3 in the right eye for which the amplitudes were the second highest. (See Table 3 for the p values of the Kruskal–Wallis test, as well as for the means and standard deviations of the mERG amplitudes in the patients and controls.) The mERG data for each group were

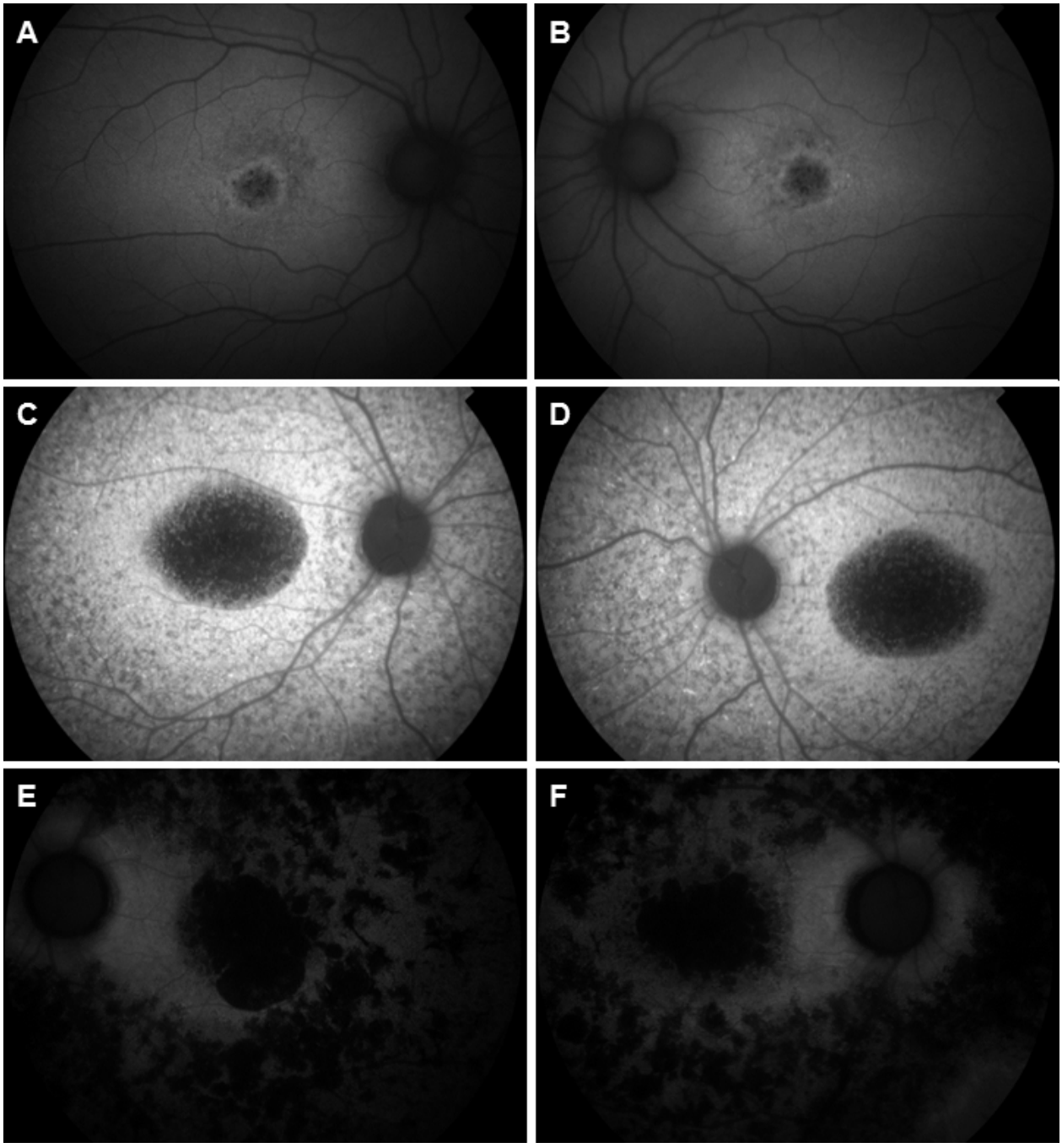

Figure 3. Representative autofluorescence images from one patient of each group. **A** and **B**: Patient 10 in group 1 shows reduced autofluorescence (AF) in the fovea with a surrounding ring of increased AF. Similar findings were encountered in all patients in group 1 except patient 1 who also demonstrated a pisciform pattern of increased and reduced AF beyond the central decreased AF. **C** and **D**: Patient 24 in group 2 shows a larger central area with the absence of AF surrounded by widespread mottling of increased and reduced AF. AF images from the other patients in group 2 are similar. **E** and **F**: Patient 30 in group 3 is in line with the other patients of the group demonstrating a large central area of absent AF, as well as widespread rounded flecks of reduced AF around the vascular arcades.

Table 2. Full-field ERG results for the different groups and controls; means ± standard deviations.

Group	Rod response (Ampl) RE, LE	Combined response a-wave (Ampl, µV) RE, LE	Combined response b-wave (Ampl, µV) RE, LE	Cone response b-wave (Ampl, µV) RE, LE	Cone response b-wave (IT, ms) RE, LE	Cone response first time b-wave (IT, ms) RE, LE
1	252±69 225±58	212±44 205±51	405±107 380±96	69±17 64±17	29.6±3.3 29.3±3.2	30.0±2.3 30.0±3.4
2	105±63 105±54	96±61 90±55	204±124 180±96	25±22 31±25	37.9±5.3 34.1±4.8	35.1±5.7 36.8±6.1
3	42±25 46±33	30±10 33±9	80±30 76±37	7±3 8±5	41.7±1.5 42.1±1.2	42.8±2.0 43.3±3.1
controls	247±59 223±58	217±52 198±50	407±89 350±85	65±22 58±16	29.9±1.6 29.5±1.	

Amp=amplitude, RE=right eye, LE=left eye, IT=implicit time, first time=first ffERG measurement in the patients that had a previous ffERG registration

also compared to the mERG results for the control group (the Mann–Whitney U-test), and statistically significantly reduced mERG amplitudes for all rings were observed in all groups and in both eyes except group 1, ring 5 left eye. P values for individual groups and rings are shown in Table 4.

Optical coherence tomography: OCT scans were captured in all patients but one (14), and retinal attenuation of some degree was found in all patients (Appendix 1). In group 1, good-quality OCT scans were recorded in 18 eyes. Only two eyes of two different patients (2 and 3; two out of 18 eyes, 11%) showed normal retinal thickness in the most central segment. For the other eyes (16 out of 18 eyes, 89%), at least the five most central segments (1–5) or more were attenuated. In two eyes (two out of 18, 11%) of two separate patients (2 and 5), all segments (1–9) were attenuated. No case of macular thickening was found. On the OCT B-scans, the photoreceptor integrity line (PIL), corresponding to the junction of the inner and outer segments of the photoreceptors, showed pathological changes in all patients. The most common alteration was a loss of PIL in the macular region (patients 1, 3–7, 9, and 10). Moreover, the PIL was totally absent in one patient (2), and a defect in a patchy pattern in the center of the macula was observed in another (8). Examples of PIL disturbances are shown in Figure 4. In group 2, OCT scans were recorded in 30 eyes (Appendix 1). Normal thickness of the most central segment was demonstrated in ten out of 30 eyes (33%) in eight patients (13, 18–20, 22–24, and 27). In those eyes, at least five, and often more, other segments were attenuated. For the remaining eyes that were measured (20 out of 30, 67%), at least segments 1–5 were attenuated. Fourteen out

Table 3. Means and standard deviations (SDs) for mERG amplitudes in rings 1–5 of each eye in the three groups of subjects as well as the p values for the Kruskal–Wallis test. For comparison, the bottom row shows means and SDs for mERG amplitudes in controls.

Group	Ring 1 (Ampl) RE LE	Ring 2 (Ampl) RE LE	Ring 3 (Ampl) RE LE	Ring 4 (Ampl) RE LE	Ring 5 (Ampl) RE LE
1	16±6 15±7	14±6 13±5	15±6 13±5	16±6 15±6	17±6 17±6
2	7±3 8±4	5±2 6±5	4±2 5±3	4±2 5±3	4±3 5±4
3	5±2 5±2	5±3 6±5	4±2 4±3	3±2 3±2	2±0,5 2±1
P value Kruskal–Wallis test	*<0,0001* *0,008*	*0,001* *0,013*	*<0,0001* *0,002*	*<0,0001* *0,001*	*<0,0001* *<0,0001*
controls	51±15 46±12	35±10 33±8	29±8 27±6	25±6 23±6	24±7 23±6

Ampl=amplitude, RE=right eye, LE=left eye

of 30 eyes (47%) in 11 separate patients (12, 15–17, 21, 22, 24–26, 28, and 29) showed thinning of all segments (1–9). Increased thickness in one peripheral segment was found in two eyes out of 30 (6.7%; patient 18, left eye, and patient 29, right eye). All patients but one (19) in group 2 demonstrated total absence of the PIL on the OCT B-scans (Figure 4). In patient 19, the PIL was missing in the macular region. In group 3, OCT scans were recorded in nine eyes. Eight of these eyes (89%; patients 30 and 32–34) showed macular thinning in at least segments 1–5, and six of the eyes (67%) showed attenuation in all nine segments. One eye of patient 31 demonstrated normal thickness in the central segment but thinning in the other segments (2–9). In group 3, the OCT B-scans showed total absence of PIL in all patients (Figure 4).

DISCUSSION

Since mutations in *ABCA4* are associated with such a wide spectrum of retinal degenerations from more localized STGD to widespread disorders, such as CRD and arRP, making a proper prognosis of visual outcome for the separate patient at the first visit is difficult but important. Therefore, in this study, we wanted to investigate the role of various electrophysiological parameters, as well as different imaging techniques and the presence of certain mutations in *ABCA4,* in the evaluation of the visual function in patients with *ABCA4*-associated retinal degenerations.

Comparison of ffERG results between the groups and to a normal material significantly demonstrated that small scotomas (group 1) are associated with normal ffERG parameters, while larger scotomas (group 2) and more extensive visual field defects that also restrict the peripheral fields (group 3) are gradually related to reduced ffERG amplitudes and with delayed ffERG cone 30 Hz flicker implicit times. The worse the visual fields were restricted, the more the amplitudes were reduced, and the implicit times were delayed. These results corroborate previous reports on ffERG in *ABCA4*-associated retinal degenerations demonstrating normal ffERG in STGD [33,34], and gradually impaired ffERG parameters in CRD [21,34,35] and arRP [14,34,35]. Concerning implicit times, a further comparison of this parameter obtained at the first visit was made to the normal material and showed that already early in the course of the disease, the implicit times were significantly prolonged in groups 2 and 3, but normal in group 1, indicating that the finding of prolonged implicit time might be used as a predictor of progressive *ABCA4*-associated retinal degenerations. Delayed ERG implicit times have been noted as an indicator of progressive conditions previously but most often in RP [36-39]. Only a few studies have described the same phenomenon in *ABCA4*-associated retinal degenerations [11,40,41]. Therefore, the present confirming survey might be of value with outcomes in line with Fakin et al. [11] showing longer implicit times in patients with progressive *ABCA4*-associated retinal degeneration compared to patients with a more stationary course of disease.

Compared to the normal material, mERG amplitudes were reduced for all groups, and significant differences in mERG amplitudes were also found between the groups. In general, group 1 with small scotomas demonstrated the least reduced amplitudes, and group 3 with widely constricted visual fields demonstrated the most reduced mERG amplitudes.

Table 4. p values for the Mann–Whitney U-test comparing mERG amplitudes of the different mERG rings in group 1–3 to the normal material. Significant p values are in italics.

mERG ring	Group 1 p values	Group 2 p values	Group 3 p values
1 RE	*<0,0001*	*<0,0001*	*0,001*
2 RE	*<0,0001*	*<0,0001*	*0,001*
3 RE	*<0,0001*	*<0,0001*	*0,001*
4 RE	*0,001*	*<0,0001*	*0,001*
5 RE	*0,010*	*<0,0001*	*0,001*
1 LE	*<0,0001*	*<0,0001*	*0,020*
2 LE	*<0,0001*	*<0,0001*	*0,005*
3 LE	*<0,0001*	*<0,0001*	*0,005*
4 LE	*0,001*	*<0,0001*	*0,005*
5 LE	0,121	*<0,0001*	*0,005*

RE=right eye, LE=left eye

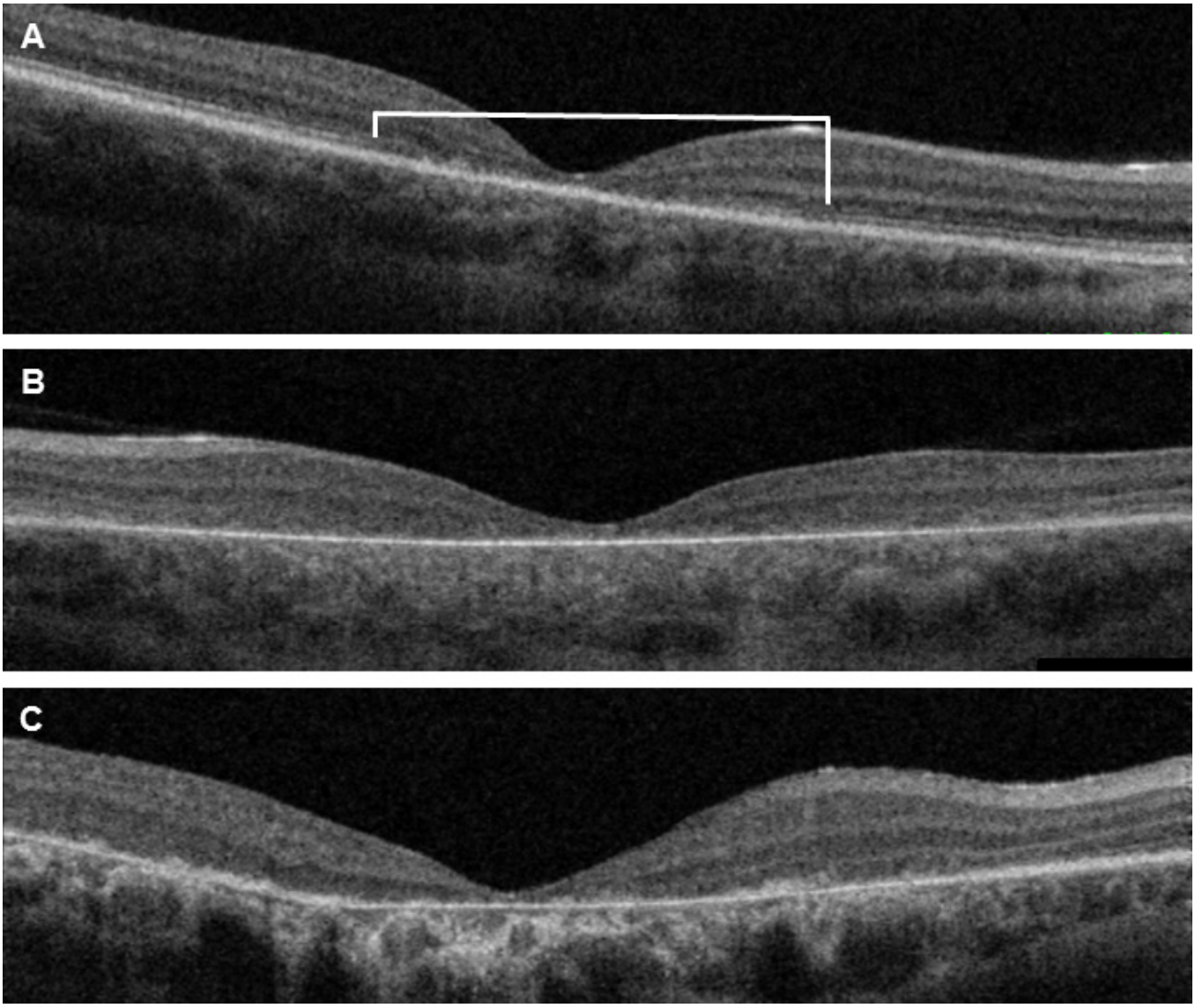

Figure 4. OCT images of one representative patient from each group. **A**: Loss of the photoreceptor integrity line (PIL; indicated by the white brace) in the macular region in patient 10 from group 1. The PIL corresponds to the junction of the inner and outer segments of the photoreceptors. The same pattern was encountered in all but two patients in group 1. One of those two patients showed more extensive PIL loss, and the other had better preserved but disorganized PIL. **B**: Representative total PIL loss and RPE atrophy in patient 24 from group 2. All but one patient in group 2 showed the same optical coherence tomography (OCT) changes. Patient 19 had a defect PIL in the center but a preserved PIL beyond this. **C**: Patient 30 from group 3 also shows total PIL loss and extensive RPE atrophy as observed in the other patients in group 3.

Changes in the retinal structure correlated well with alterations in retinal function. OCT images of group 1 showed PIL changes limited to the central macular area corresponding to electrophysiological results with normal ffERG parameters but reduced mERGs, while groups 2 and 3, with reduced ffERG parameters in addition to more widely reduced mERGs, demonstrated extensive changes in the PIL engaging the entire field of view of the OCT also beyond the macula with visibly worse changes in group 3.

Defect PILs (IS/OS junctions) have been described in *ABCA4*-associated retinal degenerations previously [11,12,33,42-44], and in some cases, the severity of ffERG and OCT changes also has shown a correlation [11,44] as in the present study. Moreover, the OCT B-scans revealed retinal attenuation in most cases, but with no typical difference between the groups, perhaps because measurement of retinal thickness with comparison to the normal database is less precise in patients with reduced VA and bad fixation. In

line with this, Testa et al. [44] showed that there is no correlation between the severity of IS/OS junctional abnormalities and retinal thickness in patients with STGD.

In addition, the AF images showed gradually more extensive changes with increasing visual field defects and more serious ERG changes. In group 1, the general AF pattern encompassed a small central area with decreased or irregular AF surrounded by a ring of increased AF with variable intensity. This agrees with findings in patients with STGD [12] and in patients with mutations in *ABCA4* that are considered to be mild and associated with normal ffERG [43]. In group 2, the central area of reduced or absent AF was generally larger and surrounded by widespread mottling or flecks of increased and reduced AF also corroborating the AF pattern in patients with abnormal ffERG and intermediate mutations in *ABCA4* reported by Fakin et al. [43]. Group 3 demonstrated large central foci of absent AF, as well as widespread confluent, rounded areas of reduced or absent AF around the vascular arcades and in the far periphery as previously described in patients with abnormal ffERG and null-like mutations in *ABCA4* [43].

Several surveys have proposed a correlation between residual ABCA4 protein activity due to the type of mutation in *ABCA4* (null mutations, splicing mutations, point mutations, etc.) and the severity of retinal degeneration [11,19,22,27,28,43], while others have opposed this hypothesis [26,29,45]. Fakin et al. [43] presented data showing that among 15 mutations in *ABCA4* combined with a known null mutation, two mutations were consistently associated with normal ffERG parameters, six were regularly associated with pathological ffERG parameters while the remaining seven mutations in *ABCA4* appeared with normal and abnormal ffERG results, highlighting the difficulty of predicting retinal function from separate mutations and combinations of mutations. In the present study, a similar phenomenon was encountered with the same mutations in *ABCA4* (e.g., c.768 G>T, c.2894 A>G, c.1331 C>T, c.5882 G>A, and c.1622 T>C) represented in all, or at least two different, visual field groups, although we were not able to standardize the mutation in *ABCA4* on the other allele in the same stringent way.

To our knowledge, this is the largest presentation of patients with *ABCA4*-associated retinal degenerations in Sweden to date. Among those patients, most patients (24/34, 71%) showed visual field defects larger than 10° indicating that mutations in *ABCA4* in the Swedish population lead to progressive forms of *ABCA4*-associated retinal degenerations in quite a large proportion of the cases. Some mutations were found more often: c.768 G >T 11 times in nine patients, c.2894 A>G six times in five patients, c.3113 C>T in five patients, and c.5882 G>A in five patients (Table 1). Homozygous mutations were most common in group 3 (3/5, 60% of the patients) compared to 2/10 (20%) in group 1 and 3/19 (16%) in group 2 leading to the suggestion that homozygous mutations might lead to more severe forms of retinal degenerations.

To conclude, assessment of retinal function with full-field and multifocal ERG, as well as investigation of the retinal structure with OCT and FAF, is valuable in the evaluation of patients with *ABCA4*-associated retinal degenerations showing corresponding and gradually more extensive changes for all modalities along with more advanced visual field defects. Additionally, in this study, normal implicit time was associated with stationary disease entities, such as STGD, while delayed ffERG implicit times, both at first visit and on follow-up, were found in the groups with the most extensive scotomas and peripheral visual field constriction indicating that prolonged implicit time might be an indicator of progressive disease. Thus, ffERG flicker implicit time might be used to predict visual outcome in *ABCA4* retinal degeneration in the beginning of the course of the disease before other signs of severe disease are apparent.

APPENDIX 1. DEMOGRAPHIC DATA, A BRIEF SUMMARY OF THE GOLDMANN VISUAL FIELDS, AND OCT FINDINGS.

To access the data, click or select the words "Appendix 1"
hom = homozygous, RE = right eye, LE = left eye, PIL = photoreceptor integrity line, temp = temporal, nas = nasal, inf = inferior, sup = superior, N = not performed

ACKNOWLEDGMENTS

We thank Ing-Marie Holst and Boel Nilsson for skillful technical assistance. This study was supported by grants from ARMEC Lindebergs stiftelse, Skåne County Council Research and Development Foundation, Stiftelsen för synskadade i fd Malmöhuslän, and Stiftelsen Synfrämjandets Forskningsfond/Ögonfonden. The authors have full control of all primary data and agree to allow the journal to review the data on request. The authors have no conflicts of interest to disclose.

REFERENCES

1. . Azarian SMTravis GH. The photoreceptor rim protein is an ABC transporter encoded by the gene for recessive Stargardt's disease (ABCR). FEBS Lett 1997; 409:247-52. [PMID: 9202155].

2. Molday LL, Rabin AR, Molday RS. ABCR expression in foveal cone photoreceptors and its role in Stargardt macular dystrophy. Nat Genet 2000; 25:257-8. [PMID: 10888868].

3. Sun HNathans J. Stargardt's ABCR is localized to the disc membrane of retinal rod outer segments. Nat Genet 1997; 17:15-6. [PMID: 9288089].

4. Hollenstein K, Dawson RJ, Locher KP. Structure and mechanism of ABC transporter proteins. Curr Opin Struct Biol 2007; 17:412-8. [PMID: 17723295].

5. Quazi F, Lenevich S, Molday RS. ABCA4 is an N-retinylidene-phosphatidylethanolamine and phosphatidylethanolamine importer. Nat Commun 2012; 3:925-[PMID: 22735453].

6. Tsybovsky Y, Molday RS, Palczewski K. The ATP-binding cassette transporter ABCA4: structural and functional properties and role in retinal disease. Adv Exp Med Biol 2010; 703:105-25. [PMID: 20711710].

7. Weng J, Mata NL, Azarian SM, Tzekov RT, Birch DG, Travis GH. Insights into the function of Rim protein in photoreceptors and etiology of Stargardt's disease from the phenotype in abcr knockout mice. Cell 1999; 98:13-23. [PMID: 10412977].

8. Kim SR, Jang YP, Jockusch S, Fishkin NE, Turro NJ, Sparrow JR. The all-trans-retinal dimer series of lipofuscin pigments in retinal pigment epithelial cells in a recessive Stargardt disease model. Proc Natl Acad Sci USA 2007; 104:19273-8. [PMID: 18048333].

9. Yamamoto K, Yoon KD, Ueda K, Hashimoto M, Sparrow JR. A novel bisretinoid of retina is an adduct on glycerophosphoethanolamine. Invest Ophthalmol Vis Sci 2011; 52:9084-90. [PMID: 22039245].

10. Mata NL, Weng J, Travis GH. Biosynthesis of a major lipofuscin fluorophore in mice and humans with ABCR-mediated retinal and macular degeneration. Proc Natl Acad Sci USA 2000; 97:7154-9. [PMID: 10852960].

11. Fakin A, Robson AG, Fujinami K, Moore AT, Michaelides M, Pei-Wen Chiang J. G EH, Webster AR. Phenotype and Progression of Retinal Degeneration Associated With Nullizigosity of ABCA4. Invest Ophthalmol Vis Sci 2016; 57:4668-78. [PMID: 27583828].

12. Gomes NL, Greenstein VC, Carlson JN, Tsang SH, Smith RT, Carr RE, Hood DC, Chang S. A comparison of fundus autofluorescence and retinal structure in patients with Stargardt disease. Invest Ophthalmol Vis Sci 2009; 50:3953-9. [PMID: 19324865].

13. Mullins RF, Kuehn MH, Radu RA, Enriquez GS, East JS, Schindler EI, Travis GH, Stone EM. Autosomal recessive retinitis pigmentosa due to ABCA4 mutations: clinical, pathologic, and molecular characterization. Invest Ophthalmol Vis Sci 2012; 53:1883-94. [PMID: 22395892].

14. Allikmets R. Simple and complex ABCR: genetic predisposition to retinal disease. Am J Hum Genet 2000; 67:793-9. [PMID: 10970771].

15. Allikmets R, Singh N, Sun H, Shroyer NF, Hutchinson A, Chidambaram A, Gerrard B, Baird L, Stauffer D, Peiffer A, Rattner A, Smallwood P, Li Y, Anderson KL, Lewis RA, Nathans J, Leppert M, Dean M, Lupski JR. A photoreceptor cell-specific ATP-binding transporter gene (ABCR) is mutated in recessive Stargardt macular dystrophy. Nat Genet 1997; 15:236-46. [PMID: 9054934].

16. Lewis RA, Shroyer NF, Singh N, Allikmets R, Hutchinson A, Li Y, Lupski JR, Leppert M, Dean M. Genotype/Phenotype analysis of a photoreceptor-specific ATP-binding cassette transporter gene, ABCR, in Stargardt disease. Am J Hum Genet 1999; 64:422-34. [PMID: 9973280].

17. Michaelides M, Hunt DM, Moore AT. The genetics of inherited macular dystrophies. J Med Genet 2003; 40:641-50. [PMID: 12960208].

18. Birch DG, Peters AY, Locke KL, Spencer R, Megarity CF, Travis GH. Visual function in patients with cone-rod dystrophy (CRD) associated with mutations in the ABCA4(ABCR) gene. Exp Eye Res 2001; 73:877-86. [PMID: 11846518].

19. Cremers FP, Van De Pol DJ, Van Driel M, Den Hollander AI, Van Haren FJ, Knoers NV, Tijmes N, Bergen AA, Rohrschneider K, Blankenagel A, Pinckers AJ, Deutman AF, Hoyng CB. Autosomal recessive retinitis pigmentosa and cone-rod dystrophy caused by splice site mutations in the Stargardt's disease gene ABCR. Hum Mol Genet 1998; 7:355-62. [PMID: 9466990].

20. Fishman GA, Stone EM, Eliason DA, Taylor CM, Lindeman M, Derlacki DJ. ABCA4 gene sequence variations in patients with autosomal recessive cone-rod dystrophy. Arch Ophthalmol 2003; 121:851-5. [PMID: 12796258].

21. Klevering BJ, Blankenagel A, Maugeri A, Cremers FP, Hoyng CB, Rohrschneider K. Phenotypic spectrum of autosomal recessive cone-rod dystrophies caused by mutations in the ABCA4 (ABCR) gene. Invest Ophthalmol Vis Sci 2002; 43:1980-5. [PMID: 12037008].

22. Klevering BJ, Deutman AF, Maugeri A, Cremers FP, Hoyng CB. The spectrum of retinal phenotypes caused by mutations in the ABCA4 gene. Graefes Arch Clin Exp Ophthalmol 2005; 243:90-100. [PMID: 15614537].

23. Martinez-Mir A, Paloma E, Allikmets R, Ayuso C, Del Rio T, Dean M, Vilageliu L, Gonzalez-Duarte R, Balcells S. Retinitis pigmentosa caused by a homozygous mutation in the Stargardt disease gene ABCR. Nat Genet 1998; 18:11-2. [PMID: 9425888].

24. Maugeri A, Van Driel MA, Van De Pol DJ, Klevering BJ, Van Haren FJ, Tijmes N, Bergen AA, Rohrschneider K, Blankenagel A, Pinckers AJ, Dahl N, Brunner HG, Deutman AF, Hoyng CB, Cremers FP. The 2588G→C mutation in the ABCR gene is a mild frequent founder mutation in the Western European population and allows the classification of ABCR mutations in patients with Stargardt disease. Am J Hum Genet 1999; 64:1024-35. [PMID: 10090887].

25. Zernant J, Lee W, Collison FT, Fishman GA, Sergeev YV, Schuerch K, Sparrow JR, Tsang SH, Allikmets R. Frequent hypomorphic alleles account for a significant fraction of ABCA4 disease and distinguish it from age-related macular degeneration. J Med Genet 2017; 54:404-412. [PMID: 28446513].

26. . Burke TRTsang SH. Allelic and phenotypic heterogeneity in ABCA4 mutations. Ophthalmic Genet 2011; 32:165-74. [PMID: 21510770].

27. Shroyer NF, Lewis RA, Allikmets R, Singh N, Dean M, Leppert M, Lupski JR. The rod photoreceptor ATP-binding cassette transporter gene, ABCR, and retinal disease: from monogenic to multifactorial. Vision Res 1999; 39:2537-44. [PMID: 10396622].

28. Van Driel MA, Maugeri A, Klevering BJ, Hoyng CB, Cremers FP. ABCR unites what ophthalmologists divide(s). Ophthalmic Genet 1998; 19:117-22. [PMID: 9810566].

29. Yatsenko AN, Shroyer NF, Lewis RA, Lupski JR. Late-onset Stargardt disease is associated with missense mutations that map outside known functional regions of ABCR (ABCA4). Hum Genet 2001; 108:346-55. [PMID: 11379881].

30. Marmor MF, Fulton AB, Holder GE, Miyake Y, Brigell M, Bach M. ISCEV Standard for full-field clinical electroretinography (2008 update). Doc Ophthalmol 2009; 118:69-77. [PMID: 19030905].

31. Mcculloch DL, Marmor MF, Brigell MG, Hamilton R, Holder GE, Tzekov R, Bach M. ISCEV Standard for full-field clinical electroretinography (2015 update). Doc Ophthalmol 2015; 130:1-12. [PMID: 25502644].

32. Sodi A, Bini A, Passerini I, Forconi S, Menchini U, Torricelli F. Different patterns of fundus autofluorescence related to ABCA4 gene mutations in Stargardt disease. Ophthalmic Surg Lasers Imaging 2010; 41:48-53. [PMID: 20128570].

33. Cella W, Greenstein VC, Zernant-Rajang J, Smith TR, Barile G, Allikmets R, Tsang SH. G1961E mutant allele in the Stargardt disease gene ABCA4 causes bull's eye maculopathy. Exp Eye Res 2009; 89:16-24. [PMID: 19217903].

34. Lois N, Holder GE, Bunce C, Fitzke FW, Bird AC. Phenotypic subtypes of Stargardt macular dystrophy-fundus flavimaculatus. Arch Ophthalmol 2001; 119:359-69. [PMID: 11231769].

35. Maugeri A, Klevering BJ, Rohrschneider K, Blankenagel A, Brunner HG, Deutman AF, Hoyng CB, Cremers FP. Mutations in the ABCA4 (ABCR) gene are the major cause of autosomal recessive cone-rod dystrophy. Am J Hum Genet 2000; 67:960-6. [PMID: 10958761].

36. Berson EL. Retinitis pigmentosa. The Friedenwald Lecture. Invest Ophthalmol Vis Sci 1993; 34:1659-76. [PMID: 8473105].

37. Berson EL, Gouras P, Hoff M. Temporal aspects of the electroretinogram. Arch Ophthalmol 1969; 81:207-14. [PMID: 5304456].

38. Hood DC, Holopigian K, Greenstein V, Seiple W, Li J, Sutter EE, Carr RE. Assessment of local retinal function in patients with retinitis pigmentosa using the multi-focal ERG technique. Vision Res 1998; 38:163-79. [PMID: 9474387].

39. Seeliger M, Kretschmann U, Apfelstedt-Sylla E, Ruther K, Zrenner E. Multifocal electroretinography in retinitis pigmentosa. Am J Ophthalmol 1998; 125:214-26. [PMID: 9467449].

40. Eksandh L, Ekstrom U, Abrahamson M, Bauer B, Andreasson S. Different clinical expressions in two families with Stargardt's macular dystrophy (STGD1). Acta Ophthalmol Scand 2001; 79:524-30. [PMID: 11594993].

41. Kjellstrom U. Association between genotype and phenotype in families with mutations in the ABCA4 gene. Mol Vis 2014; 20:89-104. [PMID: 24453473].

42. Burke TR, Fishman GA, Zernant J, Schubert C, Tsang SH, Smith RT, Ayyagari R, Koenekoop RK, Umfress A, Ciccarelli ML, Baldi A, Iannaccone A, Cremers FP, Klaver CC, Allikmets R. Retinal phenotypes in patients homozygous for the G1961E mutation in the ABCA4 gene. Invest Ophthalmol Vis Sci 2012; 53:4458-67. [PMID: 22661473].

43. Fakin A, Robson AG, Chiang JP, Fujinami K, Moore AT, Michaelides M, Holder GE, Webster AR. The Effect on Retinal Structure and Function of 15 Specific ABCA4 Mutations: A Detailed Examination of 82 Hemizygous Patients. Invest Ophthalmol Vis Sci 2016; 57:5963-73. [PMID: 27820952].

44. Testa F, Rossi S, Sodi A, Passerini I, Di Iorio V, Della Corte M, Banfi S, Surace EM, Menchini U, Auricchio A, Simonelli F. Correlation between photoreceptor layer integrity and visual function in patients with Stargardt disease: implications for gene therapy. Invest Ophthalmol Vis Sci 2012; 53:4409-15. [PMID: 22661472].

45. Gerth C, Andrassi-Darida M, Bock M, Preising MN, Weber BH, Lorenz B. Phenotypes of 16 Stargardt macular dystrophy/fundus flavimaculatus patients with known ABCA4 mutations and evaluation of genotype-phenotype correlation. Graefes Arch Clin Exp Ophthalmol 2002; 240:628-38. [PMID: 12192456].

Articles are provided courtesy of Emory University and the Zhongshan Ophthalmic Center, Sun Yat-sen University, P.R. China. The print version of this article was created on 4 January 2018. This reflects all typographical corrections and errata to the article through that date. Details of any changes may be found in the online version of the article.